Integration of CNT-based actuators for bio-medical applications – Example printed circuit board CNT actuator pipette

R. Addinall*[1], T. Sugino[2], R. Neuhaus[1], U. Kosidlo[1], F. Tonner[1], C. Glanz[1], I. Kolaric[1], T. Bauernhansl[1], K. Asaka[2]

Abstract—**In order to strengthen the position of CNT actuator technology and fasten the transfer of scientific results into application development and market introduction scientific institutes AIST Kansai and Fraunhofer IPA cooperated in the field of electroactive polymers.**

Automated dosing of small amounts of liquids normally involves quite large pipettes and motors for pipette actuation. Miniaturized pipettes can enable new areas, in which micro dosing is demanded and could be particularly beneficial in the field of medical or (bio-) chemical applications.

The approach was the direct integration of a bending CNT actuator into a PCB design, which enables a frictionless induction of movement onto a liquid. The driving electronics control the actuator with a low voltage and can be placed on the same PCB.

The result is a smooth, tailorable dispensation of liquid from the pipette with the ability to integrate the pipette into a fully automated system.

I. Introduction

Carbon nanotube (CNT) actuators have always presented several advantages over materials currently in use – piezo ceramics and shape memory alloys. They can offer higher work per cycle than previous actuator technologies and generate much higher mechanical strength. Additionally, CNTs require very low driving voltages for their operation what in many cases presents the major advantage. Another benefit is the direct conversion of electrical energy to mechanical energy followed by high actuation strain, high strength, high elastic modulus and low density. These features can be utilized in such applications as micro pumps, molecular motors or nano robots.

AIST Kansai was the first organisation to publish the results on the development of so called "dry" carbon nanotube actuators [1], whereas Fraunhofer IPA was the first to disclose a functional model demonstrating applicability of those actuators in macro scale devices [2].

The first development resulting from this cooperation is a miniaturized pipette in which the carbon nanotube actuator developed by AIST Kansai was integrated by Fraunhofer IPA with the help of FEM simulation and printed circuit board (PCB) manufacturing methods.

The concept entails that if a small volume of air can be displaced by an integrated actuator when external electrical stimuli is applied, the change in volume and thus pressure within the connected channel will enable the movement (sucking and release) of liquid.

* Corresponding Author

1 Fraunhofer Institute for Manufacturing Engineering and Automation, Nobelstrasse12, 70569 Stuttgart, Germany.
Ivica.kolaric@ipa.fraunhofer.de

2 Health Research Institute, National Institute of Advanced Industrial Science and Technology (AIST), Midorigaoka 1-8-31, Ikeda, Osaka 563-8577, Japan

II. Computer simulation

Using simulation techniques, many relevant material and performance parameters can be obtained and investigated under real-life conditions without the need to conduct large test series or build multiple prototypes. The main reason for using simulation technology in this field was the shared wish of the partners to be able to predict the actuation performance of various pipette geometries in order to optimize shapes for individual applications and enhance the actuation mechanism through mechanical leverage effects. However, the actuation mechanism of CNT actuators is based on a very complex interaction of several chemical and quantum physical effects (quantum chemical-based expansion due to electrochemical double-layer charging) [3]. This complexity has not only hindered but in fact prevented the use of simulation technology in CNT actuator related design activities due to the lack of computational models that comprise all relevant effects.

A. Parameter matching

One approach to model the actuation characteristics of the CNT actuators used is to match experimental data with the theory of common linear elastic models. A parameter correlation has been performed at IPA to transfer existing measurement data from AIST about voltage/displacement and force relationships of CNT actuators into a set of virtual material parameters usable for simulation environments.

The actuator part of the pipette consists of two CNT-electrodes separated by an electrolyte spacing layer. In the ANSYS Workbench simulation environment, the actuation of the electrode material is initiated by a virtual thermal load applied to all parts of the simulation assembly. The thermal load causes the electrodes to expand and to shrink, respectively. The lower electrode is modelled with a negative thermal expansion coefficient, the upper electrode is attributed with a positive thermal expansion.

For a 2.5V voltage applied, the forceless displacement measurements at AIST yielded an effective value for medium electrode strain of 0.9 %, which has been modelled with a isotropic thermal coefficient of expansion of 0.00023/K and a virtual temperature difference 39 K. This value is independent of the Young's modulus. The estimation of a Young's modulus for simulation is essential for matching the measured actuation forces with the simulated actuation forces. For the AIST electrode material, a fitted Young's modulus of 42MPa was found. The real Young's modulus has been estimated using a Zwick tensile testing machine. It was found to be very non-linear. The graph below shows a small modulus for small displacements, a maximum for medium displacements and generally a plastic behavior (hysteresis in cycle).

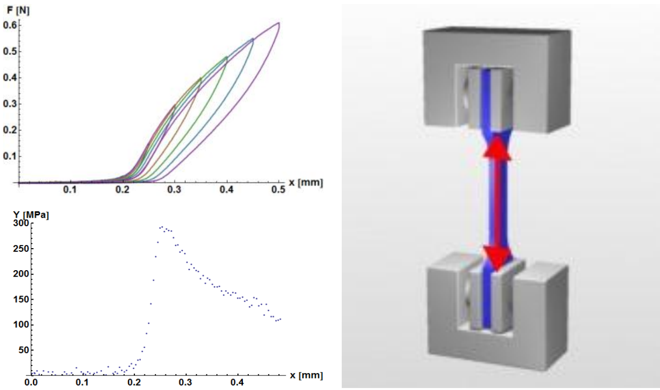

Figure 1 - Tensile characterization of CNT-electrodes. Top: Force over displacement for several load cycles; Bottom: Local slope of force over displacement (non-linear Young's modulus); Right: Illustration of a Zwick testing machine.

The Young's Modulus to be used within the simulation was obtained through iteratively comparing the simulated forces with the measured forces. The actual non-linear characteristic of the material was thus circumvented. The actuation is now directly coupled with the virtual temperature. A temperature sweep will result in a displacement sweep, imitating different voltages applied to the electrodes.

B. *Geometry optimization*

To simplify future mass-production and to keep down production costs it is deemed beneficial to combine this actuation technology with present-day PCB technology. Standardized interfaces and production enable easy integration of driver electronics, and the mechanical properties of PCB components can be used for optimizing the actuator performance, i.e. increase the bending displacement and thus the dispensed fluid volume.

The macro-scale actuation performance depends strongly on the mechanical build-up of the non-rigid electrode layers and the interface to their rigid attachment base. Figure 2 shows the design evolution for achieving maximum displacement with minimum complexity of electrode attachment and little material effort.

The improved setup contains a flexible membrane with a circular or square-shaped perforation in the middle. The two actuating electrodes are firmly attached to the rim of the membrane perforation on the top side, covering the membrane perforation and thus closing the top surface of the future pipetting chamber. This configuration was implemented into the Ansys 15.0 simulation environment. Two versions were investigated: One with a circular membrane perforation and a circular electrode attachment area, one with a square-shaped membrane perforation and a square-shaped electrode attachment. For different sizes of the membrane diameter/edge-length and the membrane perforation diameter/edge-length, the resulting displacement has been simulated in order to find the best geometry.

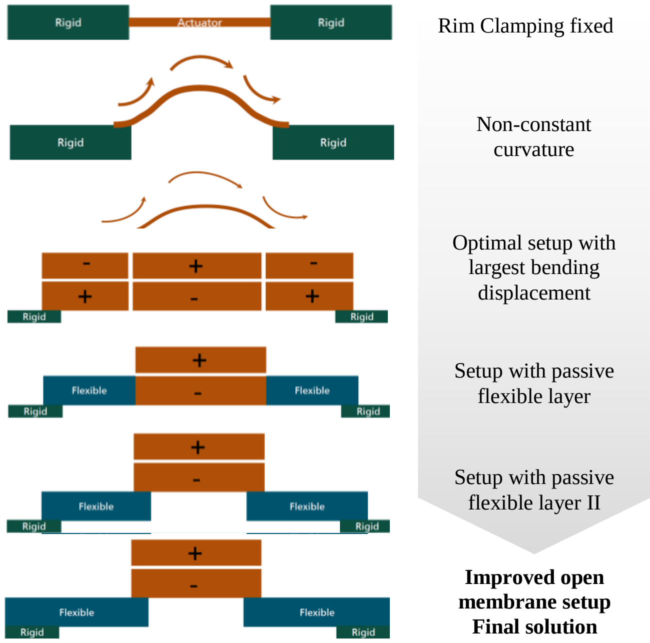

Figure 2 – Design evolution for actuator electrode attachment on rigid PCB base for optimum displacement

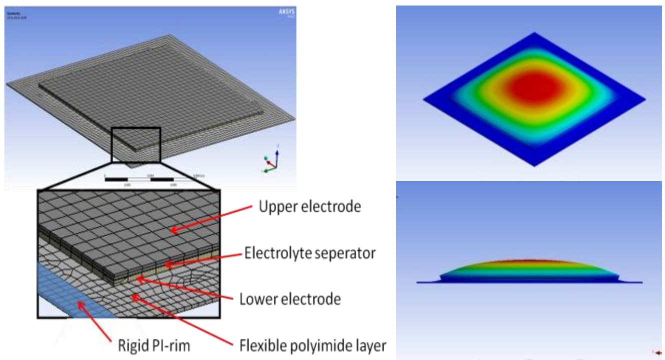

Figure 3 – Left: meshed design model of the square-shaped actuator version for displacement simulation using Ansys Workbench; right: simulation result for displacement of the model indicating a smooth curvature of the actuating membrane (20x to scale)

Table 1 and 2 illustrate the results for the displacement of the round and square-shaped pipettes with both versions of membrane material, polyimide foil (Kapton) and PTFE (Teflon).

Outer diameter of flexible layer	Actuator diameter	Hole diameter in flexible layer	Deformation z-direction in [µm] Polyimide	PTFE
16	14	12	238,89	305,33
14	12	10	216,11	277,80
12	10	8	188,07	246,48
10	8	6	155,91	208,83
8	6	5	116,21	185,09

Outer length of flexible layer	Actuator Length	Length of hole in flexible layer	Deformation z-direction in [µm] Polyimide	PTFE
18	16	14	114,12	164,56
16	14	12	101,83	148,37
14	12	10	88,37	130,49
12	10	8	73.98	110,61
10	8	6	58,23	88,32

Table 1 – Simulation results for deformation values of various square- and round-shaped electrode geometries

III. EXPERIMENTAL PROCEDURE

A. Electrode material and construction of actuators

The single-walled CNTs (SWCNTs) from Unidym (Purified HiPco®) was used as a carbon source. Polyaniline (PANI) (20 wt% polyaniline on carbon black) (Sigma-Aldrich Co.) was used as a conductive additive. 1-Ethyl-3-methylimidazolium tetrafluoroborate ($EMIBF_4$) (Tokyo Chemical Industry Co., Ltd.) and polyvinyliden fuluoride-co-hexafluoroborate (PVDF-HFP: Kynar Flex2801) (Archema Chemical Inc.) were used as an internal and a base polymer, respectively. A typical experimental procedure to prepare the electrode and electrolyte films of actuators is mentioned below [4], [5].

50.4 mg (12.0 wt%) of SWCNTs, 50.0 mg (11.9 wt%) of PANI, 240.1 mg (57.1 wt%) of $EMIBF_4$, and 80.0 mg (19.0 wt%) of PVDF-HFP were dissolved into 9 mL of N,N-dimethylacetamide (DMAc). The mixture was stirred for more than 1 day at room temperature, then sonicated in an ultrasonic bath for 24 hours. A black gelatinous mixture was obtained after sonication. The self-standing electrode films were obtained by casting and drying the black gelatinous mixture. The opaque self-standing electrolyte films were obtained from a 1:1 weight ratio mixture of $EMIBF_4$ and PVDF-HFP by a similar casting method. The CNT actuators have three-layered structure where an electrolyte film is laminated with two electrode films by heat-pressing.

B. PCB manufacturing

Printed circuit boards (PCB) technology was chosen as suitable integration material due to the flexibility in design that PCBs offer. In this particular case it refers to flexibility in integration of sensor, contacts, the various material substrates (Polyimide, PTFE, etc.) as well as the flexibility and ease in manufacturing of more complex geometries if needed.

The PCB boards were made of standard FR4 material. Multiple variations of PCB pipettes were constructed with several design variations (see Table 2); one main focus of the joint activities of AIST Kansai and Fraunhofer IPA is the integration of the actuator into the PCB and a comparison between the different shapes and dimensions and their respective influence on the overall actuation performance.

	Shape of electrode fixation and soldered contact layer	Shape of dispenser-tip	Shape of liquid compartment
Version #1	Round	Un-pointed	Round
Version #2	Round	Pointed	Round
Version #3	Square	Un-pointed	Round
Version #4	Square	Pointed	Round
Version #5	Round	Un-pointed	Square

Other material and shape parameters	
Young's modulus for electrode layers	42 MPa
Flexible layer thickness (passive layer)	0.05 mm
Thickness of actuator electrodes	150 µm
Thickness of electrolyte layer	15 µm

Table 2 – Overview of the different PCB versions manufactured and list of fixed geometrical electrode parameters

Standard 50 µm polyimide foil (Kapton) was used for the first prototypes. Half of the second shipment involved Teflon (PTFE) as membrane material for investigating the influences of different friction coefficients, Young's Moduli and densities of the flexible membrane. The channel geometry of the pipette was chosen to be 1 mm x 1mm x 10 mm (depth milled into 1.5 mm FR4). The diameter of the pipette chamber was 20 mm. Copper contacts were added in order to directly contact the PCB substrates to the actuator. Figure 4 shows the layer stacking schematics for the PCB manufacturing, figure 5 shows the PCB-design schematics in EDA Altium Designer software and the finished cover-PCB.

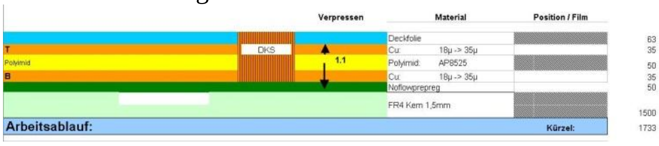

Figure 4 – Layer stack for PCB of pipette.

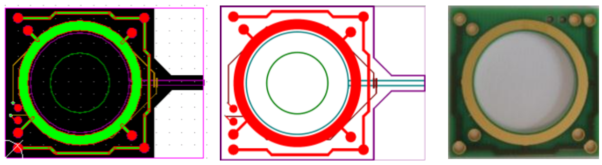

Figure 5 – EDA (Electronic design automation) drawings of pipette PCB showing the fluid channel linking the round compartment in the center with the outlet tip. Right: finished cover-PCB

C. System integration

For attaching the actuator onto the PCB board, several adhesive materials were tested in order to determine which group of bonding agents meets the requirements of good gluing performance, easy handling, low cost and good temperature stability. The most appropriate would then be used for the system integration of the AIST actuator to the PCB pipette model.

Adhesive	Active/ hazardous Ingredient	Viscosity (mPa s)	Temperature stability (°C)	Main component
Tool craft super glue	cyanoacrylate	NA	0 to 50°C	Ethyl-2-cyanoacrylate
Universal glue extra	N'-(3-aminopropyl)-N,N-dimethylpropane-1,3-diamine	400000	-20 to 125	Neoprene
UHU plus two part	Aliphatic amines	40000 (binder) 30000 (hardener)	-40 to 80	Epoxy Resin

Table 3 – Types and properties of adhesive materials investigated

However, it turned out that none of the liquid adhesives were suitable for the actuator integration. The double sided tape (3M IF-7953MPL) supplied by Inno Tape GmbH was subsequently used. This specialized double sided adhesive tape not only enabled faster system integration but also ensured a defined adhesion thickness. Two geometries were produced for the attachment of the actuator to the flexible passive membranes: Disk shaped double sided tapes were stamped out for the attachment of the actuator to the closed passive membrane, whereas ring shaped geometries, which were laser cut, where used for the open flexible membrane. In both cases (open and closed membrane) the tape was placed in the middle, the actuator positioned on top and a defined pressure was applied.

As illustrated in Figure 6, the counter PCB (green) was tape glued (PVC electric insulation tape or clear scotch tape) to the bottom part of the PCB/actuator setup. This was made for both the closed and the perforated (open) flexible membrane setups.

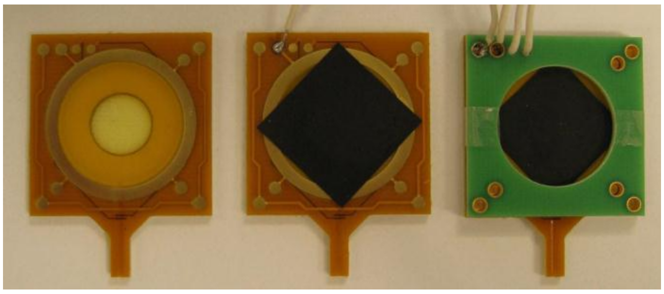

Figure 6 – PCB of pipette (left) in raw form, (middle) covered with CNT actuator and (right) with cover PCB.

Electrical wiring was soldered to the respective contacts integrated within the PCB board in order to attach the pipette to an external voltage supply.

D. Test setup

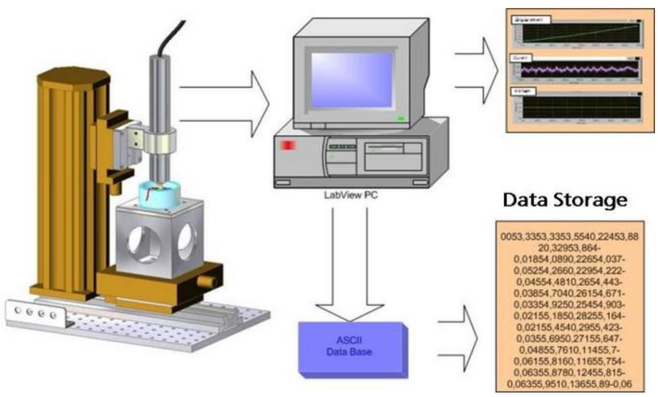

Figure 7 – Displacement measurement setup envisaged

A set up similar to the illustration above (Figure 7) was used to measure the vertical displacement of the integrated actuator. The constant parameter was voltage and was set at 2V for all actuator displacement tests. The measurement system (opto NCDT 2400 from MICRO-EPSILON) consisted of passing monochromatic light onto the top surface of the integrated actuator. The spectral changes induced by the reflected light (interferometry) enabled the precise measurement of the displacement of the actuator.

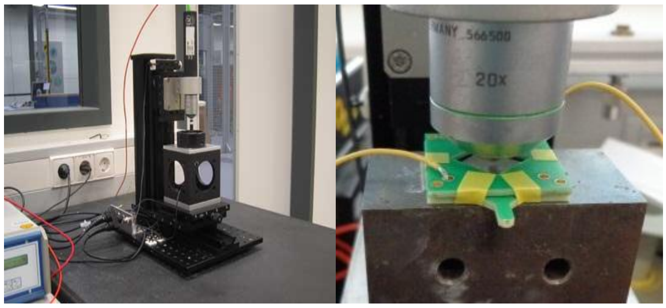

Figure 8 – Displacement measurement setup used. Monochromatic light (left) and white light (right) interferometry

IV. RESULTS AND DISCUSSION

Regarding the actuation mechanism, the application of voltage of different polarity at each side of the actuator caused one of the carbon nanotube layers to expand and the other one to contract [6]. The proton exchange membrane between the top and bottom layers enabled movement of ions while isolating electron flow. This resulted in the bending of the whole structure.

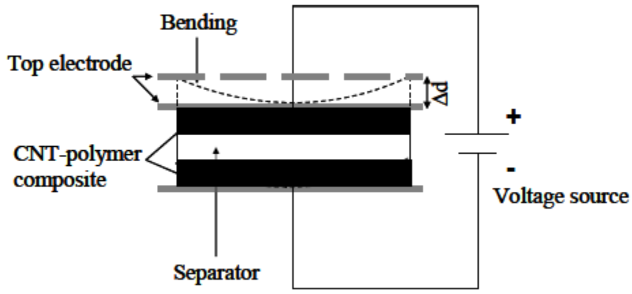

Figure 9 – Sketch of actuating mechanism

The displacement tests proved that all the actuators integrated within the PCB pipette functioned, however with varying degrees of performance.

Although there was a difference in vertical displacement (up and downwards movement) the results were all within a reasonable range. In order to better understand what mechanisms could influence the actuation leading to a change in upwards and downwards movement infrared imagery was used to depict hot spots created by possible short circuits caused during the integration of the actuator to the PCB pipette [7].

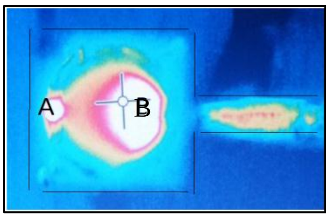

A = Hot spot through potential short circuit
B = Expected hot area due to actuation mechanisms

Figure 10 – infrared imagery of integrated actuator showing joule heat generation within the actuator electrodes during 2V operation

As the concept of a pipette actuator consists of collecting and dispensing liquid, after the initial Interferometry tests the pipette was used in conjunction with liquid media.

The first batches of tests were made using distilled water, which proved very successful as movement of liquid was observed. Upon closer observation, and although a drop of liquid had formed at the end of the nozzle connected to the chamber, the surface tension of the distilled water proved to be too high to enable the liquid bubble to drop. Due to this fact, a second batch of tests was made using a mixture of water and acetone (75:25% or 3:1). This had the effect of lowering the surface tension and helped generate a larger drop on the end of the pipette. Finally, the drop actually dropped or detached itself from the nozzle, however this result was not reproducible. A third batch of solution was made consisting of copper sulphate solution, this was mainly employed to reinforce the contrast between the drop and background by adding a bluish tint to the solution but also to provide conductivity of the fluid to be detected via the included electrodes.

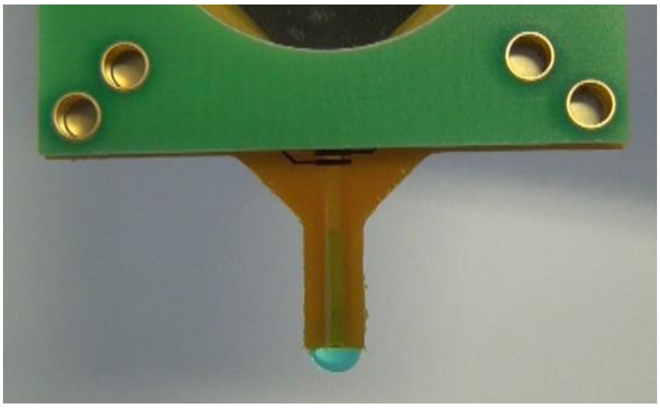

Figure 11 – Drop formation of copper sulphate solution

Using a LCR meter at 1 kHz measurement frequency and a saturated solution of copper sulphate (approx. 17 g in 50 ml water) in Millipore water, the detection electrodes integrated into the dispensing channel have shown to read a change in resistance during the dispensing process. For several cycles of filling and depleting, the detection electrodes showed continuous readings of resistance ranging from 330 Ohm to 675 Ohm.

V. Conclusion

The integration of carbon nanotube actuator technology into application of miniature pipette is in the first place beneficial in the field of micro dosing in medical or (bio-) chemical applications. The demonstrated model offers a compact and energy efficient system with advantage of precise dosing. In a next step, integration of many pipettes into microfluidic control systems offers further extension of current development, and will creation of the "Lab-on-a-PCB" systems for precise and controlled handling of small volumes of liquid. But that is just a beginning and the results of this first demonstration can be transferred to further fields of applications where the advantages of CNT actuators can be utilised for functions such as precise switching, positioning and manipulation.

Acknowledgment

References

[1] T. Fukushima, K. Asaka, A. Kosaka, T. Aida, "Fully plastic actuator through layer-by-layer casting with ionic-liquid-based buckey gel", Angew. Chem. Int. Ed., 44, 2005, 2410-2413.

[2] Kosidlo, U., Addinall, R., Tonner, F., Glanz, C., Kolaric, I., Bauernhansl, T., "Improvement of the CNT Actuator Reproducibility by Means of Process Simplification" International Union of Materials Research Societies -IUMRS-; Materials Research Society of Japan, Tokyo; International Conference on Electronic Materials (ICEM), Yokohama, Japan, 23.-28., September 2012

[3] S. Geier, J. Riemenschneider, T. Mahrholz, P. Wierach, M. Sinapius; "Investigations of the key mechanism of Carbon-Nanotube Actuators and their dependencies" Institute of Composite Structures and Adaptive Systems, DLR e.V. (German Aerospace Center), Braunschweig, Germany

[4] T. Sugino, K. Kiyohara, I. Takeuchi, K. Mukai, K. Asaka, "Improving the actuating response of carbon nanotube/ionic liquid composites by the addition of conductive nanoparticles", Carbon, 49, 2011, 3560-3570.

[5] T. Sugino, Y. Shibata, K. Kiyohara, K. Asaka, "CNT/conductive polymer composites for low-voltage driven EAP actuators", Proceedings of SPIE 8340: 63400T-1-8.

[6] K. Kiyohara, T. Sugino, I. Takeuchi, K. Mukai, K. Asaka, "Expansion and contraction of polymer electrodes under applied voltage", J. Appl. Phys., 105, 2009, 063506-1-8. Erratum: J. Appl. Phys., 105, 2009, 119902-1.

[7] Kosidlo, U., Addinall, R., Tonner, F., Kolaric, I., Glanz, C., "Experimental investigations on carbon nanotube actuators defining the operation point and its standard deviation" Smart Structures and Materials + Nondestructive Evaluation and Health Monitoring 2010: Electroactive Polymer Actuators and Devices (EAPAD) 2010, Ed. Yoseph Bar-Cohen, Proc. Of SPIE Vol. 7642, 76421B